ORIGINAL ARTICLE

Kinetic studies of Congo red dye adsorption by immobilized *Aspergillus niger* on alginate

Mohammed T. M. H. Hamad[1] · Mona S. S. Saied[1]

Abstract

Releasing of dye-containing wastewater by the textile industry into general water bodies can adversely affect aquatic ecosystems and human health. The objective of this study is to assess the Congo red dye biodegradation and detoxification by immobilized *Aspergillus niger* obtained from textile dye wastewater. The effects of process parameters like pH, temperature, reaction time and initial concentration on Congo red degradation were studied. Equilibrium adsorption isotherms, kinetics and thermodynamics were also investigated. The experimental data were analyzed by the Langmuir, Freundlich and Temkin models of adsorption. The adsorption isotherm data fitted well to Langmuir isotherm and the kinetic data fitted well to the pseudo-second-order model. The degraded metabolites of Congo red were characterized by using UV–Vis spectrophotometer, Fourier transform infrared spectroscopy and high-performance liquid chromatography, further confirmed that biodegradation of Congo red was due to reduction of the azo bond. Phytotoxicity test confirmed that degradation metabolites were a less toxic than original dye. The reusability of the immobilized *Aspergillus niger* was repeated with six cycles and removal efficiency ranged from 98 to 72%. The results in this study substantiate that immobilized *Aspergillus niger* could be employed as a good adsorbent for the removal of Congo red dye from wastewater.

Keywords Congo red · Fungal strain · Degradation · Phytotoxicity

Introduction

Developed countries are facing many challenges, such as the limited freshwater resources, increasing food demand, rising population, industrial activities 'pollution and stress linked to change in climate conditions. To overcome these challenges, reuse of treated wastewater may be one of the most promising practical solution for reducing the gap between current water demand and supply (Niemczynowicz 1999). Textile of many industries such as paper, cosmetics, rubber, plastic, leather, food, photo graphical and pharmaceutical purposes are containing a variety of dyes and auxiliary chemicals that consume a huge amount of water each day and produce large quantities of wastewater that contain many hazardous compounds. These industries withdraw their wastes to the water bodies affecting badly on the groundwater system and interrupts the aquatic environment which

causes adverse impact on phytoplankton's photosynthesis and may be toxic to aquatic life itself (Siegel 2002; Ho et al. 2012). EL-Alamiadye company located at Cairo Governorate uses about 1.2 millions of cubic meters of water for a monthly output of around 8000 kg of the finished product (Khan et al. 2013). The application of Azo Dye in textile industry represents 60–70% of all the dyes used (Senan et al. 2004). Using textile wastewater containing azo dyes in the crops irrigation process can change the biological properties of soil including the composition of microbial communities and enzyme activities (Muhammad et al. 2014). The synthetic dyes are classified to Azo, anthraquinone, heterocyclic polymers and triphenylmethane dyes (Yang et al. 2009). Most of Azo dyes have their resonance and π-conjugated Azo bond characteristics, so it is resistant to degradation by microorganisms, temperature, light, heat, water, detergents, and bleach (Lade et al. 2015). Azo dyes are mutagenic and carcinogenic to humans as well as some animals due to cleavage of the Azo bond to aromatic amine can stereo chemically transform to an electrophile compound that forms covalent bonds with DNA and deteriorates the DNA double helical structure (Whitehead et al. 2009). Congo

✉ Mohammed T. M. H. Hamad
  mohammedtaha2010@outlook.com

[1] Central Laboratory for Environmental Quality Monitoring,
  National Water Research Center, Cairo, Egypt

red is one of the common azo dyes, which has two Azo bonds (–N=N–) connected to aromatic rings, that is used in the textile industry (Konstantinou et al. 2004). It consists of a sodium salt of benzidinediazo-bis-1- naphtylamine-4 sulfonic acid (Bentahar et al. 2016). It is highly soluble in water and organic solvents such as ethanol, and persistent once discharged into a natural environment (Jalandoni-Buan et al. 2009; Giovinazzi et al. 2011). Benzidine is a product of the cleavage of Congo red which is a human carcinogen and mutagen (Asses et al. 2018). Currently, it is a big challenge to treat dye wastewater by chemical and physical processes due to its complex molecular structures (Buthelezi et al. 2012). These methods involve chemical oxidation using various oxidants, e.g., ozone (Wu et al. 2017), Fenton reagent (Hameed et al. 2009), electrochemical oxidation (Moghaddam et al. 2015), catalytic reduction (Shanmugam et al. 2015), photocatalytic degradation (Rahimi et al. 2012), microwave (Kato et al. 2010), chemical adsorbents (Yang et al. 2009) such as silica (Shaw et al. 2011) and activated carbon (Ahmad et al. 2014), but these conventional methods usually have passed many challenges as high cost chemicals and equipment, low adsorption, large amount of sludge production and requiring high energy (Hetnarski et al. 2009). In last decades, many studies have focused on bioremediation methods. Bioremediation methods are including bacteria, yeasts, filamentous fungi and microalgae, which have the ability to catalyze the degradation of various toxic chemicals to less harmful forms (Popli et al. 2015). The advantages of using a microbial method in decolorization dye are because of its cheap production, less harmful environmental impact, simple equipment, less energy, eco-friendly materials and diverse microorganisms with various metabolic products. White-rot fungi and their extracellular enzymes are one of the best methods for the removal of synthetic dye-containing wastewater (Gnanadoss et al. 2013). In previous studies, *Aspergillus terreus, Rhizopus oligosporus* and *Aspergillus flavus* have been used a lot to remove azo dyes (Asses et al. 2018). Nowadays, the technology of immobilized fungal cells is being increasingly used in industrial application wastewater treatment due to several advantages which are more resilient to environmental perturbations such as pH, or exposure to toxic chemical concentrations, mechanical

strength, chemical stability, cost effective, physical morphology, long retention time, anti-degradation ability and cell viability for several cycles of operations (Wesenberg et al. 2003). Immobilization of microbial cells within the polymeric matrices such as chitosan, chitin, cellulose derivatives and calcium alginate has been studied widely. Immobilized fungal biomass *Aspergillus niger* on the charcoal activated carbon was successfully applied to decolorize Methylene Blue (RB), Reactive Black 5, Congo Red and Malachite Green which are azo dyes commonly used in the industrial processes (Alam et al. 2018). Chitosan-immobilized *Rhizopus arrhizus* was used to decolorize Cibacron Turquoise HGN (CT) and Remazol Red RGB (RR). Bentonite, as an adsorbent material, is the most widely used one due to its naturally availability, good action exchange capacity, high surface area, micro-porous structure, and less cost (Alam et al. 2018). For all these advantages, this work focuses on two main objectives to investigate the potential of immobilized fungi for decolorization and degradation of textile Congo red dye.
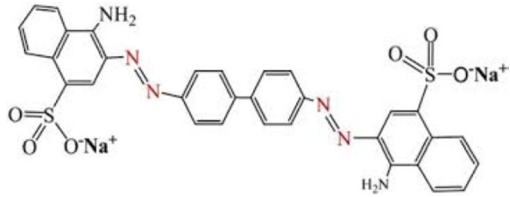
Materials and methods

Chemicals

Congo red Table 1 (the sodium salt of benzidinediazo-bis-1- naphthylamine-4-sulfonic acid C32H22N6Na2O6S2; molecular weight, 696.66 g/mol) and 3- ethylbenzthiazoline-6-sulfonic acid were purchased from Hi Media Laboratories Pvt. Ltd. (Mumbai, India).The media such as Sabroud dextrose agar (SDA) and Sabroud Dextrose broth (SDB) were obtained from Oxoid.

Isolation of fungi

The fungi were isolated from textile industrial wastewater samples that were collected, according to the Standard Methods for the Examination of Water and Wastewater, APHA (Rice et al. 2012), from the 10th Ramadan textile Company, Egypt. One mL of effluent was added to 9 mL of distilled water in sterile test tubes to prepare the stock solution. 1 mL

Table 1 The characteristics of Congo red dye

Dye	Chemical structure	Molecular weight	Class
Congo red		696,66	Diazo

from this stock solution was spread on Sabroud Dextrose Agar (SDA) plates with the help of L-rod. The petri plates were incubated at 30 °C for 5 days. Pure fungal isolates were obtained on the SDA plates by sub-culturing. The isolates were further sub-cultured on SDA slants and incubated at 30 °C. After sufficient growth of the colonies, the slants were stored in refrigerator and served as stock cultures. Every 30 days sub-culturing were routinely done.

Decolourization assay

The mineral salt medium (MSM) used for decolourization studies composed of 5 mg glucose, 1 mg KNO_3, 0.3 mg KH_2PO_4, 0.7 mg $MgSO_4$, 1 mg K_2HPO_4. The dye was added at a concentration of 100 mg/L. The MS medium containing Congo red dye was autoclaved at 121 °C for 15 min. Each organism in flasks (containing dye) was incubated at 30 °C with shaking 140 rpm for 36 h. Dye decolourization activity was expressed in terms of percentage decolourization. Fungal culture with dye in MSM was filtered for the removal of biomass. The degree of decolourization of the dye was measured at its respective maximum absorbance wavelength (500 nm) for Congo red using supernatant by UV–visible spectrophotometer. The decolourization assay was calculated according to the following formula.

$$Biodecolourization \% = \frac{A° - A}{A°} \times 100 \qquad (1)$$

where A° and A are the absorbance of the concentrations of the dye before and after biodecolourization, respectively (Ramya et al. 2007).

The identification of decolorized fungi by 16SrRNA technique

The 16SrRNA partial sequencing analysis was carried out in order to identify the highest decolorizing fungal isolate of Congo red. The universal primers ITS1 (5′ TCC GTA GGT GAA CCT GCG G 3′) and ITS4 (5′ TCC TCC GCT TAT TGA TAT GC 3′) were used to amplify the 16S rRNA. The sequenced data that obtained were subjected to blast analysis using public database Gene Bank at www.ncbi.nlm.nih.gov/BLAST suggesting the identity of isolates. The sequences were aligned the CLUSTAL W program and analyzed with the MEGA 7.0 software16. The phylogenetic tree was constructed using Maximum Likelihood method with bootstrap values was calculated from 1000 replicate runs (Megha et al. 2015).

Immobilization of decolorized fungi by sodium alginate

The following solutions were prepared by dissolving 2.5 g of sodium alginate in 100 mL distilled water, 1.5 g of bentonite in 100 ml distilled water and 2.5 g of calcium chloride in 100 ml distilled water, then all solutions were autoclaved at 121 °C for 15 min and then cooled. For immobilization of fungi after culturing in sabroud dextrose broth, fungal cells were harvested by centrifugation (45,000 rpm for 20 min), the 10 g pellets, sodium alginate and bentonite solutions were mixed together and stirred. This mixture was extruded by micropipette into the 100 mL calcium chloride with continuous stirring. The formed beads were removed from calcium chloride solution and rinsed with phosphate buffer. The samples were refrigerated for 48 h (Kumar et al. 2014).

UV–visible and FTIR analyses

Color reduction was assayed by absorbance measurements 340–500 nm using a UV/VIS spectrophotometer (Aqua Meta 80000, Thermo Scientific). After culture centrifugation at 4500 rpm for 15 min, the supernatants were analyzed by measuring the absorbance differences. FTIR analysis of lyophilized fungal biomass was monitored on a Jasco FTIR-8400S, USA. The FTIR spectra were then recorded between 625–4000 cm^2.

Gas chromatography–mass spectrometry (GC–MS)

GC–MS analysis was carried out using an Agilent 7890A Series GC system coupled with Agilent 5975c Inert Mass Selective Detector, USA. Degradation products were identified by comparison of fragmentation patterns, as well as with the fragmentation products detected in Congo red degradation process (Chhowalla et al. 2013).

Phytotoxicity bioassay

Effect of Congo red dye solution and treated dye solution was studied on lentils seed germination. Ten lentils seeds were watered everyday with 50 ml of distilled water as control, Congo red dye and treated dye solutions separately. The experiment repeated three times and was conducted at room temperature of 28 ± 1 °C. Percent of germination and the lengths of shoot and root were recorded during 14 days (Skouteris et al. 2015).

Recycling experiments for immobilized fungus

Congo red decolourization studies were performed six times to assess the reusability of immobilized fungus for an initial concentration of 100 mg/L. Before each cycle, the pieces

were washed six times with sterile water to remove any unattached dye. Congo red decolourization experiments were performed at 30 °C for 30 h for each cycle.

Results and discussion

A total of 11 fungal isolates were isolated from textile effluent samples and screened for their potential to decolorize Congo red from liquid medium. One isolate was selected for further studies based on its ability to degrade Congo red from liquid medium efficiently and rapidly showing more than 98.8% decolourization Fig. 1. Based on comparing between 16S rRNA sequence of *Aspergillus niger* and valid species in Gen Bank using MEGA 7 software, the decolorized fungus was identified by 16S rRNA technique as *Aspergillus niger*. Phylogenetic tree analysis was constructed based on neighbor joining tree method as illustrated in Fig. 2. The database was deposited in NCBI GenBank under the accession number MK640786.

Structural analysis

Gas chromatography–mass spectrometry (GC–MS)

The various metabolites obtained during the biodegradation process of Congo red by *Aspergillus niger* MK640786 were analyzed by GC–MS. Figure 3 shows various display degradation product at different retention times. Chemical structures were compared to the National Institute of Standards and Technology (NIST) library. The GC-mass spectra detected four peak of treated Congo red dye by *Aspergillus niger* MK640786 at retention time 4.036 min (Gentamicin) with peak area 3.45%, 21.996 min(Rhodopin peak)with area
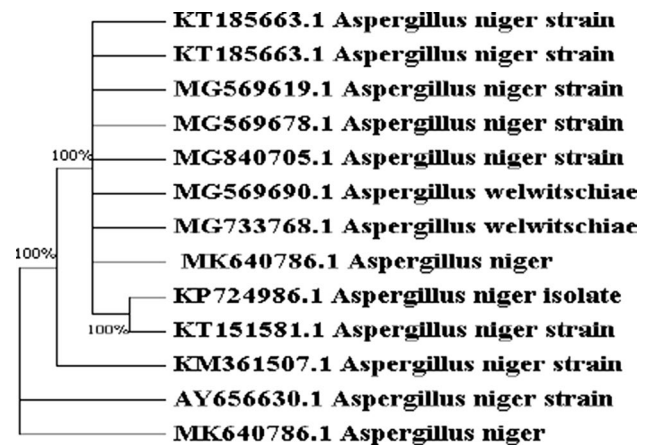

Fig. 2 Phylogenetic tree of *Aspergillusniger* (MK640786) constructed with neighbor joining method using MEGA 7 software

9.02%, 22.68 min (Cholestane-3,5-diol, 5-acetate) with peak area 8.08%, 24.379 min (cis-11-Eicosenoic acid) with peak area16.93% and 23.728 min (cis-11-Eicosenoic acid) with peak area 79.45%.The first step in the microbial degradation of azo dyes was a cleavage of electrophilic azo bonds by azo reductase and laccase enzymes to form aromatic amines as end products and most of amines further get degraded by the actions of oxidative enzymes (Dave et al. 2015).

Phytotoxicity test

Disposing untreated textile effluents into the water bodies may cause serious environmental and health risks. Thus, it was of high concern to evaluate the phytotoxicity of the dye before and after degradation. The mean shoot and root lengths of the Lentils plant were 2.3 ± 0.2 and
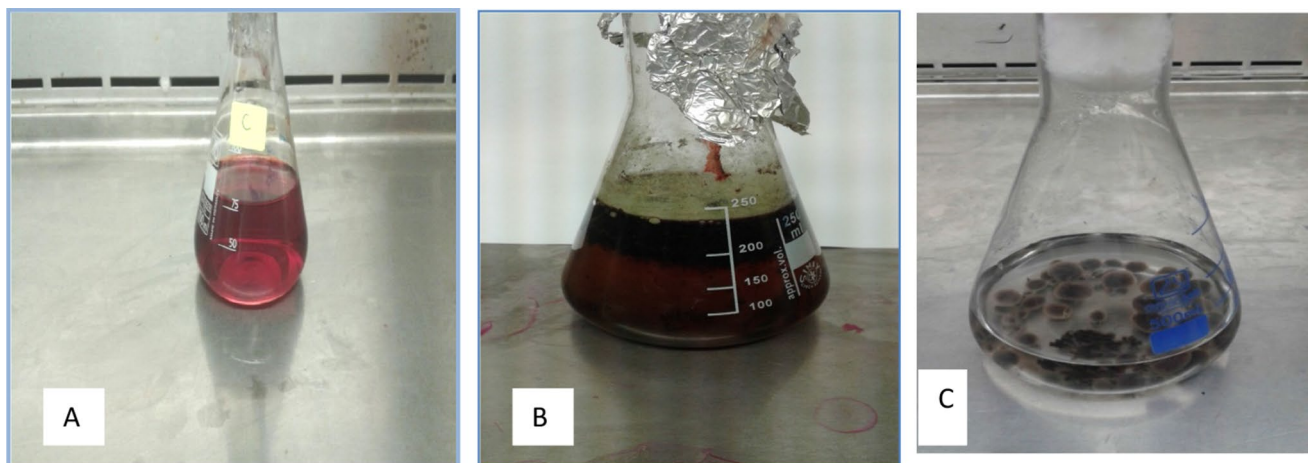
Fig. 1 Photographs of decolourization of Congo red (CR) dye. **a** Congo red dye (Control). **b** Degraded congo red dye by *Aspergillusniger* (MK640786). **c** Immobilization of decolorized fungi by sodium alginate
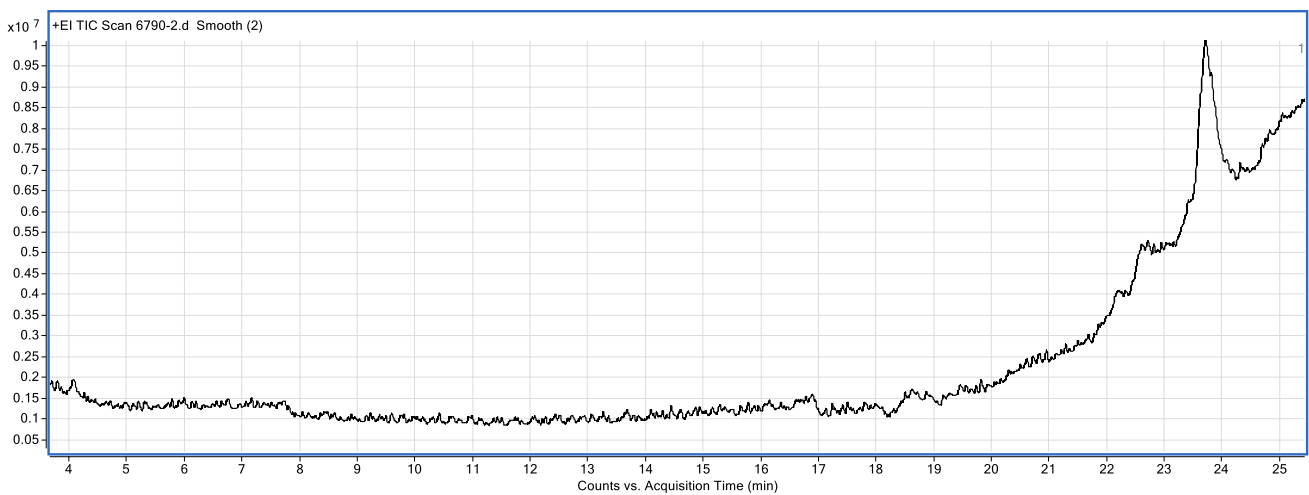
Fig. 3 GC–MS spectra of Congo red after treatment with *Aspergillusniger*

Fig. 4 Phytotoxicity study of CR before and after biodegradation by *A. niger on* Lentils

0.16 ± 0.005 cm, respectively, after treatment with untreated Congo red dye, while the mean shoot length and root length were 3.2 ± 0.02 and 0.13 ± 0.01 cm after treatment with the treated effluent during 14 days, respectively. The plant that was treated with distilled water, as a positive control, showed a shoot length and a root length equals 5.1 ± 0.2 and 0.31 ± 0.01 cm during14th days, respectively (Fig. 4, Table 2). Asses et al. (2018) also found that germination rate of the Zea mais, when wetted with Congo red treated solution, was less as compared with its degradation products and distilled water.

Recycling experiments for immobilized fungus

The operational stability of strain *Aspergillus niger* MK640786, reactions was performed to examine the

Table 2 Phytotoxicity of Congo red before and after biodegradation

Parameters	Distilled water (as a control)	Congo red before treatment	Congo red after treatment
Germination (%)	100%	40%	80%
Mean shoot length (cm)	5.1 ± 0.2	2.3 ± 0.02	4.1 ± 0.1
Mean root length (cm)	0.31 ± 0.01	0.16 ± 0.01	0.31 ± 0.01

recycling of the immobilized fungus. Effective decolourization was observed up to six cycles of 100 mg of Congo red dye. In the first cycle, 98% of the dye was decolorized in 30 h. During the six cycles, the efficiency was decreased to 72% decolorization. The results obtained are shown in Fig. 5. Similar observations have been recorded previously
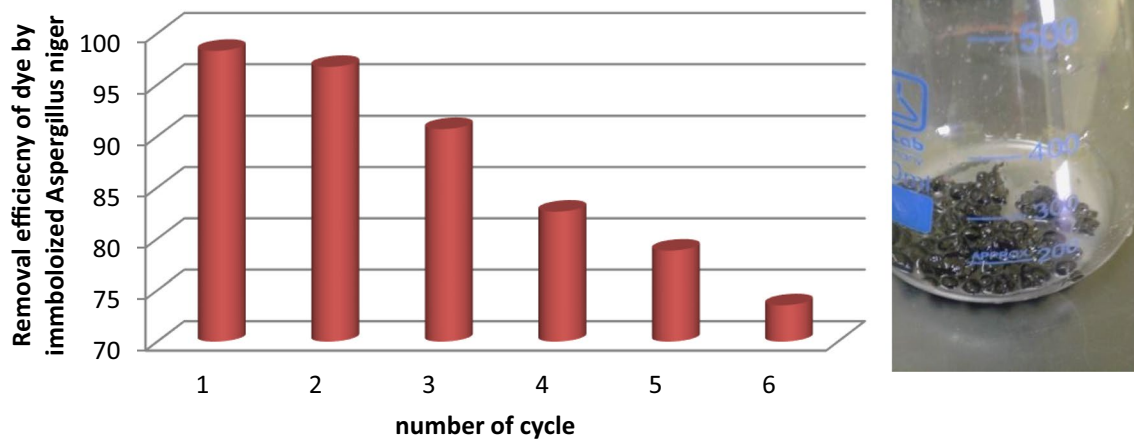
Fig. 5 Number of reusability of immobilization fungi in sodium alginate for removal dye
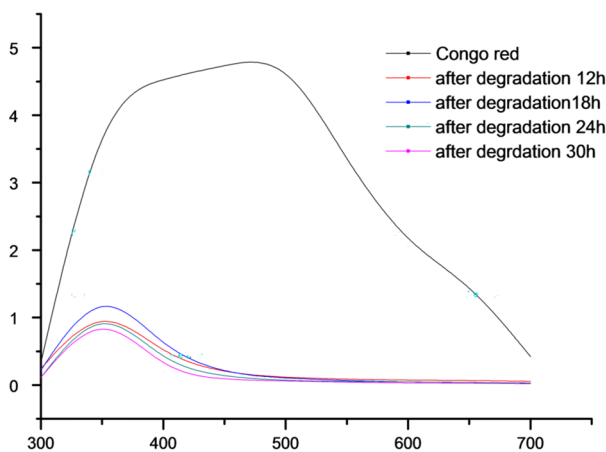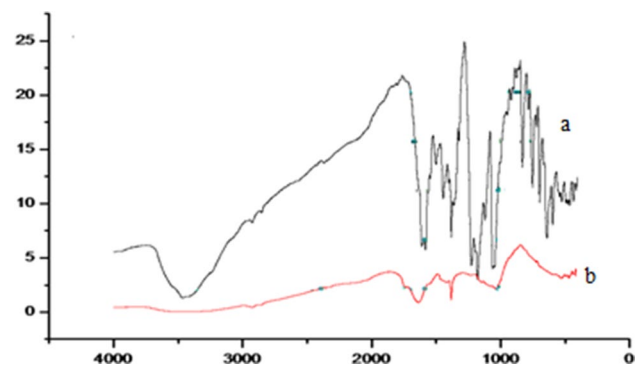

Fig. 6 UV–visible absorption spectrum of Congo red before and after CR decolorization

Fig. 7 FTIR spectra of inactive *A. niger* before (**a**) and after biosorption of CR dye (**b**)

UV–visible analysis

Decolourization of the control Congo red at time zero and Congo red dye sample mixed with *Aspergillus niger* MK640786 at different time periods was confirmed by UV–visible analysis and is depicted in Fig. 6. There are two peaks observed at 340 and 490 nm for untreated dye at zero time. Decolourization of CR was confirmed by the decrease in the intensity of dye peak in proportion with time. After enzymatic degradation, the peaks were gradually decreased without a change in λ max before disappearing. The absence of the main peak at 490 nm after 36 h as well as the minor peak at 340 nm indicates that the *Aspergillus niger* was able

for the decolourization of Congo Red by alginate entrapped on Turnip (Brassica rapa) during more than 4 cycles (Ahmedi et al. 2015).

to cleave the azo bond of CR dye and to form the aromatic amines (Asses et al. 2018).

Fourier transform infrared analysis

Figure 7 represents a comparison of FTIR spectra of *Aspergillus niger* before and after the biosorption of Congo red dye.Fig. 7 shows specific strong band peak at 3465 cm^{-1} due to the bounded OH groups, while the peak observed at 2921 cm^{-1} was due to the C=H asymmetric stretching group. The peak at 1799 cm^{-1} was attributed to the stretching vibrating carboxyl group. The bands at 1610 and 1419 cm^{-1} were attributed to asymmetric and symmetric stretching vibration of C–O groups. The C=N stretching band was observed at 1326 cm^{-1}. Bands at 1178 and 1049 cm^{-1} were assigned to C=O stretching of alcohols and carboxylic acids. The hydroxyl or amine groups of stretching vibration bands at 3465 cm^{-1} was appeared less intensity after Congo red adsorption. The stretching band of C–H groups was shifted from 2923 to 2925 cm^{-1}.The stretching band of carboxyl groups was shifted from 1799 to

1743 cm^{-1}. The bands around 1193 cm^{-1} represent the tertiary amine group and also not found in degraded dye metabolite. The aromatic rings, at 1402 cm^{-1}, were also not found in the degraded dye products. The stretching bands at 1610 and 1464 cm^{-1} were also shifted to 1635 and 1419 cm^{-1}, respectively. The stretching band at 1382 cm^{-1} shows peak reduction with less intensity. The C=O peaks at 1178 and 1049 cm^{-1} were shifted to 1041 and 723 cm^{-1}, respectively.

Adsorption experiments

The effect of initial dye concentration

The initial dye concentration has a very important impact for the water treatment system; it specifies the maximum concentration with the higher removal percentage that can be treated by a specific amount of the adsorbent. The adsorption of different dye concentrations (from 50 to 250 mg/L) was examined by adding a specific adsorbent dose (10 mg) to the same solution volume (50 mL) for a specific long contact time (1800 min) without any change in the pH values. At the end of the equilibrium period, the adsorbent was removed from the solution by filtration (using an automatic filtration system) with the suitable filtration paper. Figure 8 illustrates the relation between the initial dye' concentrations, in mg/L, and the corresponding removal percentage. In general, the removal increases gradually with concentration till the equilibrium concentration after which the removal percentage decreases as extra dye ions have no available space to be adsorbed in and remain in the solution. The equilibrium concentration of Congo dye is 150 mg/L. The removal efficiency is 88%.

The effect of pH on the dye removal

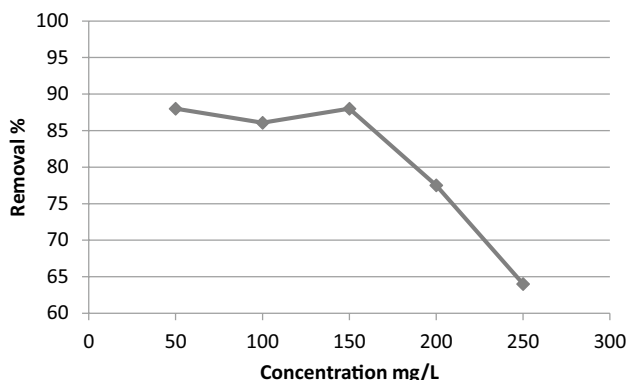Dye sorption is critically linked with pH, each dye shows different optimum pH for its sorption. The pH value of the dye prepared solution before adding the adsorbent dose is pH 7. The effect of pH change has been investigated in the range of 5–9 as shown in Fig. 9. It was found that the highest removal percentage (about 99%) was at pH 5, and the percentage decreases with the increase in the pH values.

The effect of contact time on the dye removal

The adsorption kinetics or contact time is one of the most important data in order to understand the mechanism of the adsorption and to assess the performance of the adsorbent. It is the time interval at which adsorption is studied. In general the rate of sorption starts fast in the beginning of the interaction between adsorbate and adsorbent and the rate of percent removal becomes almost insignificant due to a quick exhaustion of the adsorption sites and to a larger surface area and pores of the adsorbent being available for the adsorption of the dye ions (Hussin 2011). Different time intervals (720:1800 min) have been studied with the concentration identified before (150 mg/L), and the dye removal percentage at each interval has been calculated Fig. 10. It is clear from the figure that the removal percentage increases with time. So, the maximum time interval (1800 min or 30 h)
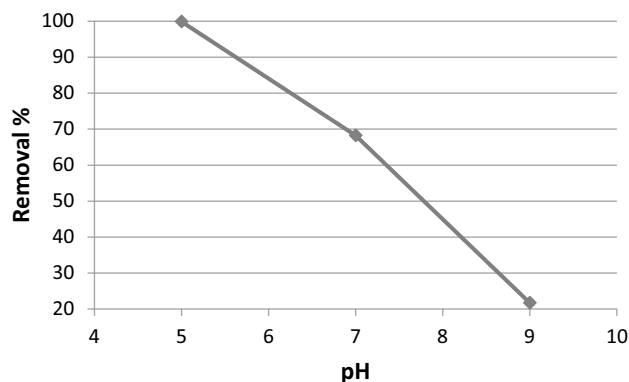
Fig. 9 pH versus removal (%) by *Aspergillus niger*

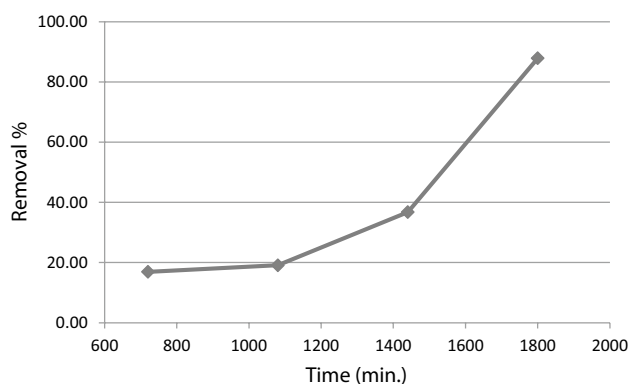**Fig. 8** Initial Congo dye concentrations versus removal (%) by *Aspergillus niger*

Fig. 10 The effect of contact time on CR removal

showed the maximum removal percentage and considered the optimum time for the adsorption process.

The effect of temperature on the metal ions removal

The effect of temperature on the considered metal ions was investigated, and the removal percentage at 298, 303, 308, and 314 K was calculated. This step is very important to understand the reaction thermodynamics. It was found that the adsorption efficiency is almost independent on temperature (ranges between 86.7 and 89.3%) and the higher removal efficiency is observed at 303 K temperature as shown in Fig. 11 (endothermic reaction).

Adsorption isotherm

The adsorption isotherm is an invaluable curve that describes the phenomenon governing the retention, release, or mobility of substance molecules from the aqueous porous media or liquid environments to a solid-phase, at a constant temperature and pH, when the adsorption process reaches an equilibrium state (Foo et al. 2010). The equilibrium data obtained in this study were analyzed in terms of three isotherms; Langmuir isotherm (Eq. 2), Freundlich isotherm (Eq. 3), and Temkin isotherm (Eq. 4).

$$\frac{C_e}{q_e} = \frac{C_e}{Q_{max}} + \frac{1}{Q_{max}K_L} \qquad (2)$$

$$\ln q_e = \ln K_F + \frac{1}{n} \ln C_e \qquad (3)$$

$$q_e = \frac{RT}{b} \ln (K_T) + \frac{RT}{b} \ln (C_e) \qquad (4)$$

where q_e (mg metal per g dry adsorbent) is the adsorption capacity of the composite, C_e is the metal ion concentration after treatment (mg/L), Q_{max} (mg/g) is the Langmuir constant related to the maximum monolayer adsorption capacity, K_L (L/mg) is the constant related to the free energy or net enthalpy of adsorption, K_F (mg/g) is the Freundlich constant that is related to the adsorption capacity, i (dimensionless) is the Freundlich exponent empirical parameter related to the intensity of adsorption (for favorable adsorption n should be in the range 1‹n‹10), K_T (L/gm) is the Temkin isotherm equilibrium binding constant, b is the Temkin isotherm constant, R is the universal gas constant (8.314 J/mol/K), and T is the room temperature (298 K).

Langmuir isotherm

The Langmuir isotherm is based on the simple assumptions that molecules are adsorbed as a saturated monolayer with a thickness of one molecule with no transmigration in the surface plane, and the interaction between adsorbed molecules is negligible with a constant adsorption energy (Roy et al. 2018).

Plotting the relation between C_e/q_e and C_e produces a straight line (R^2 is too close to 1) that satisfies with good agreement the Langmuir isotherm as shown in Fig. 12. The essential feature of the Langmuir isotherm model can be expressed in terms of 'R_L' a dimensionless equilibrium parameter, which is defined by Eq. 5:
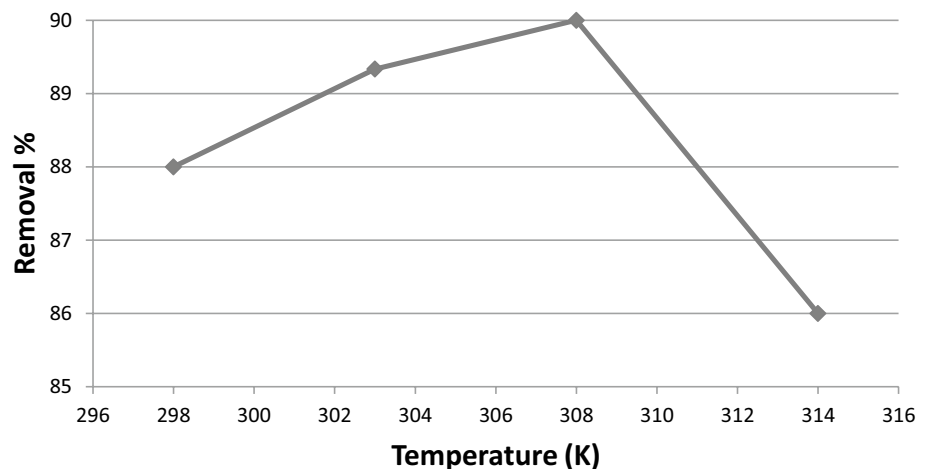
$$R_L = \frac{1}{1 + K_L C_o} \qquad (5)$$

where C_o (mg/L) is the initial amount of adsorbate and K_L (L/mg) is the Langmuir constant described above. The R_L parameter is considered as more reliable indicator of the adsorption. There are four probabilities for the R_L value:

For favorable adsorption $0 < R_L < 1$,
For unfavorable adsorption $R_L > 1$,
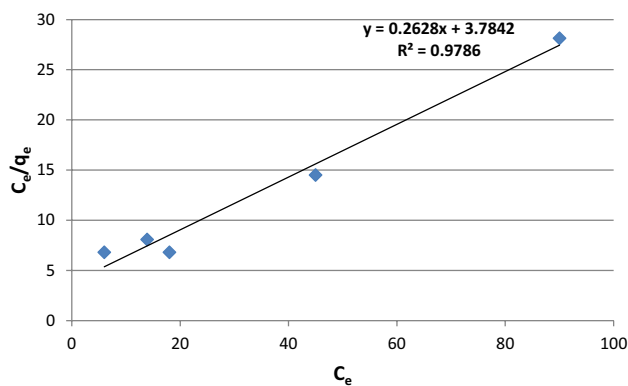
Fig. 11 The effect of temperature on CR removal

Fig. 12 C_e/q_e versus C_e for Langmuir isotherm application

Fig. 13 $\ln(q_e)$ versus $\ln(C_e)$ for Freundlich isotherm application

For linear adsorption $R_L = 1$ and
For irreversible adsorption $R_L = 0$.

From the slope and intercept of the straight line, the Langmuir isotherm constants (Q_{max}, K_L, and R_L) are calculated Table 3. Comparing the values of q_e (measured experimentally) and Q_{max} (calculated), it is clear that they are close to each other, which confirm the application of the equation.

Freundlich isotherm

It is an empirical equation based on the assumption that the exchanger surface is heterogeneous as well as multilayer adsorption and that each class of exchange sites adsorbs individually according to the Langmuir isotherm. It is derived by assuming an exponentially decaying adsorption site energy distribution (Roy et al. 2018).

By drawing the relation between $\ln C_e$ and $\ln q_e$ Fig. 13, the Freundlich and exponent constants (K_f and i) are calculated from the intercept and slope of the straight lines. The calculated Freundlich isotherm constants and the corresponding coefficients of correlation values are shown in Table 4. The coefficient of correlation was not high (R^2 value is 0.8817) indicating a bad linearity. So, this model could not be applied in case of using *Aspergillus niger* for the adsorption CR dye.

Temkin isotherm

By ignoring the extremely low and large value of concentrations, the model assumes that heat of adsorption (function of temperature) of all molecules in the layer would decrease linearly rather than logarithmic with coverage. As implied in

Table 4 Constants of Freundlich isotherm for the adsorption of CR dye by *Aspergillus niger*

Parameter	R^2	Slope	Intercept	n	K_f
Value	0.805	0.462	− 0.709	2.163	0.492

Eq. 4, its derivation is characterized by a uniform distribution of binding energies (Dada et al. 2012).

By drawing the relation between q_e and $\ln C_e$ Fig. 14, the Temkin isotherm equilibrium binding constant and the Temkin isotherm constant (A_T and b) are calculated from the intercept and slope of the straight line. The calculated Temkin constant and the corresponding coefficient of correlation values are shown in Table 5. The coefficient of correlation was not high enough to verify the model concepts (R^2 value is 0.868).

Kinetics of Congo Red removal over *Aspergillus niger* fungus

The best-fit equations of linear and nonlinear forms of the two widely used kinetic models, namely pseudo-first-order (PFO) and pseudo-second-order (PSO) equations, have been applied in this study.

The adsorption of adsorbed ions from an aqueous solution onto the adsorbents can be considered as a reversible linear process with equilibrium being established between the solution and the adsorbent. Lagergren's first-order rate equation has been so-called pseudo-first-order kinetics: The pseudo-first-order model is expressed as (Lin et al. 2009).

Table 3 Constants of Langmuir isotherm for the adsorption of CR dye by *Aspergillus niger*

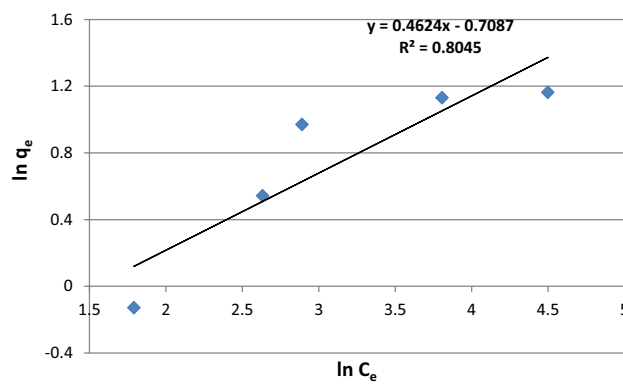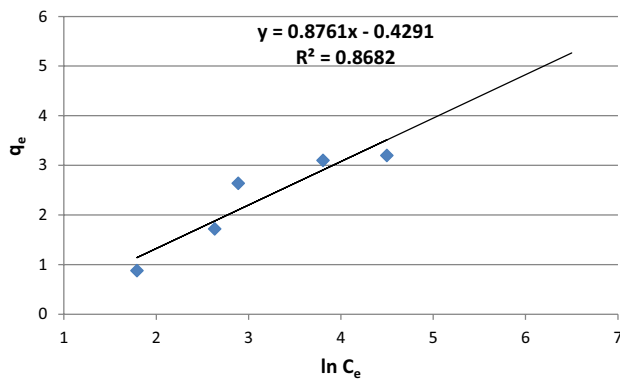| Parameter	R^2	Slope	Intercept	q_e (mg/g)	Q_{max} (mg/g)	K_L (L/mg)	R_L
Value	0.979	0.2623	3.784	3.200	3.805	0.056	0.088

Fig. 14 q_e versus lnC_e for Temkin isotherm application

Table 5 Constants of Temkin isotherm for the adsorption of CR dye by *Aspergillus niger*

Parameter	R^2	Slope (B)	Intercept	A_T	b
Value	0.868	0.876	-0.429	0.613	2827.956

$$\log \left(q_e - q_t\right) = \log q_e - \left(\frac{k_1}{2.303}\right)t \tag{6}$$

where k_1 is the rate constant of pseudo-first order (min^{-1}). q_e and q_t refer to the amount of dye adsorbed at equilibrium and at time (t), respectively. On the other hand, when the process becomes nonlinear, it is called: pseudo-second-order model is expressed as (Lin et al. 2009).

$$\frac{t}{q_t} = \frac{1}{k_2 q_e^2} + \frac{1}{q_e}t \tag{7}$$

where k_2 is the pseudo-second order rate constant of adsorption, q_e and q_t refer to the amount of dye adsorbed at equilibrium and at time (t), respectively. The validity of each model was checked by the fitness of the straight line (R^2) as well as the consistence between experimental and calculated values of q_e.

Pseudo-first-order (PFO) model for Congo red sorption.

Plotting the relation between log ($q_e - q_t$) versus t, to apply the pseudo-first-order model, is presented in Fig. 15 and the corresponding parameters (R^2, slope, intercept, rate constant of pseudo-first-order model "K_1", and experimental and calculated dye uptake amounts) are illustrated in Table 6. As it is clear, R^2 values not close to unity to be suitable to express the sorption process. Also, the experimental and calculated q_e values are not alike or even close to each other that confirm the achieved result.
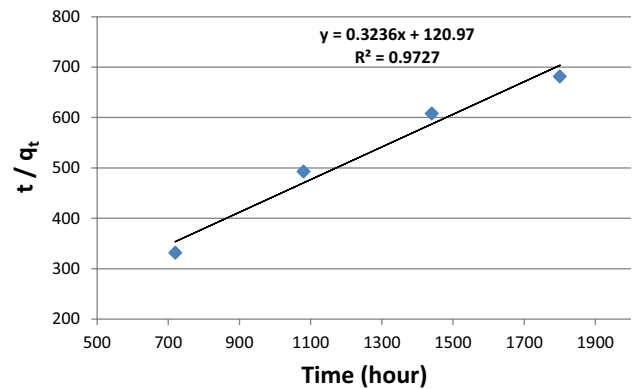
Fig. 15 PSO model application for CR on *Aspergillus niger* fungus

Pseudo-second-order (PSO) model for Congo red sorption

The plot of t/q_t versus t gave a straight line as shown in Fig. 15, from its intercept and slope, the values of K_2 and R^2 are evaluated Table 7. The applicability of the model was examined by evaluating the correlation coefficient (R^2) and the matching between the experimental and calculated q_e values. From Table 6, the R^2 value is close to unity, and the experimental and calculated q_e values are close to each other. So certainly, PSO model can be applied for the sorption of the dye ions.

The chemical thermodynamics

The thermodynamic parameters of the adsorption reaction and the values of K_L (Langmuir constant described before) at different temperatures were processed according to the following Van't Hoff equation (Tapabashi et al. 2019)

$$\ln K_L = \frac{-\Delta H^{\circ}}{RT} + \frac{\Delta S^{\circ}}{R} \tag{8}$$

where ΔH° and ΔS° are enthalpy and entropy changes, respectively, and R is the gas constant. Plotting ln K_L against $1/T$ gives a straight line with a slope and an intercept equal to $\Delta H^{\circ}/R$ and $\Delta S^{\circ}/R$, respectively, from which enthalpy and entropy changes can be calculated.

The Gibbs free energy (ΔG°) of adsorption was calculated from the following relation:

$$\Delta G^{\circ} = \Delta H^{\circ} - T\Delta S^{\circ} \tag{9}$$

Table 8 shows the thermodynamic parameters of the reaction. The enthalpy change is positive indicating that the reaction is an endothermic one, and from the ΔG° values we can deduce that the process is a non-spontaneous one.

Table 6 Constants of PFO model for the adsorption process

Parameter	R^2	Slope	Intercept	K_1	Exp. q_e	Cal. q_e
Value	0.671	− 0.002	1.824	0.005	2.650	66.700

Table 7 Constants of PSO model for the adsorption process

Parameter	R^2	Slope	Intercept	K_2	Exp. q_e	Cal. q_e
Value	0.973	0.324	120.970	0	2.650	3.090

Table 8 The chemical thermodynamic parameters for the sorption of CR on *Aspergillus niger*

Parameter	T (K)	ΔH (kJ/mol)	ΔS (kJ/mol K)	ΔG (kJ/mol)
Value	298	50,732.028	144.414	7696.602
	303			6974.531
	305			6252.461
	314			5385.975

Conclusion

The application of conventional wastewater treatment consumes hug chemical materials which becomes uneconomical and causes further environmental risks. The removal of Congo red is primarily controlled by the dye concentration, adsorbent concentration, pH, and the temperature of the adsorption process. The percentage of dye removal was found to increase with an increase in reaction contact time, and adsorbent concentration. Equilibrium data were fitted to Langmuir isotherm. The kinetics of the adsorption process was found to follow the pseudo-second-order kinetic model. The thermodynamic parameters indicate that the adsorption process is endothermic and non-spontaneous in nature. The study concluded that the Congo red dye could be degraded with up to 98.8% by *Aspergillus niger,* at optimum conditions as follows: 10 g adsorbent, pH 5, 150 mg/L initial dye concentration, and 308 K temperature for 200 mL volume of solution. These results are recommendable of using economically and eco-friendly immobilized fungal techniques to be applied for decolorizing industrial wastewater.

Compliance with ethical standards

Conflict of interest The authors declare that they have no conflict of interest.

References

Ahmad M et al (2014) Biochar as a sorbent for contaminant management in soil and water: a review. Chemosphere 99:19–33. https://doi.org/10.1016/j.chemosphere.2013.10.071

Ahmedi A et al (2015) Effect of diffusion on discoloration of Congo red by alginate entrapped turnip (Brassica Rapa) peroxidase. Enzyme Res. https://doi.org/10.1155/2015/575618

Alam MZ et al (2018) Development of an effective biosorbent by fungal immobilization technique for removal of dyes. Waste Biomass Valoriz 9(4):681–690. https://doi.org/10.1007/s12649-016-9821-9

Asses N et al (2018) Congo red decolorization and detoxification by *Aspergillus Niger*: Removal mechanisms and dye degradation pathway. Biomed Res Int. https://doi.org/10.1155/2018/3049686

Bentahar Y et al (2016) Adsorptive properties of Moroccan clays for the removal of arsenic (V) from aqueous solution. Appl Clay Sci 119:385–392. https://doi.org/10.1016/j.clay.2015.11.008

Buthelezi SP et al (2012) Textile dye removal from wastewater effluents using bioflocculants produced by indigenous bacterial isolates. Molecules 17(12):14260–14274. https://doi.org/10.3390/molecules171214260

Chhowalla M et al (2013) Goki Eda, Lain-Jong Li, Kian Ping Loh, and Hua Zhang. Nat Chem 5:263. https://doi.org/10.1038/nchem.1589

Dada A et al (2012) Langmuir, Freundlich, Temkin and Dubinin-Radushkevich isotherms studies of equilibrium sorption of Zn2+ unto phosphoric acid modified rice husk. IOSR J Appl Chem 3(1):38–45. https://doi.org/10.9790/5736-0313845

Dave SR et al (2015) Bacterial degradation of azo dye containing wastes. Microbial degradation of synthetic dyes in wastewaters. Springer, Berlin, pp 57–83

Foo K et al (2010) Insights into the modeling of adsorption isotherm systems. Chem Eng J 156(1):2–10

Giovinazzi S et al (2011) Lifelines performance and management following the 22 February 2011 Christchurch earthquake. N Z Highlights Resil. https://doi.org/10.5459/bnzsee.44.4.402-417

Gnanadoss JJ et al (2013) Decolourization of synthetic dyes using free and immobilized *Aspergillus* species. Res Biotechnol 4(5):20–23

Hameed B et al (2009) Degradation of malachite green in aqueous solution by Fenton process. J Hazard Mater 164(2–3):468–472. https://doi.org/10.1016/j.jhazmat.2008.08.018

Hetnarski RB et al (2009) Thermal Stresses: Advanced Theory and Applications. Springer, Berlin

Ho Y et al (2012) Industrial discharge and their effect to the environment. Ind Waste. https://doi.org/10.5772/38830

Jalandoni-Buan AC et al (2009) Congo red decolorizing activity under microcosm and decolorization of other dyes by Congo red decolorizing bacteria. Philipp J Sci 138(2):125–132

Kato MT et al (2010) Effect of iron on matrix metalloproteinase inhibition and on the prevention of dentine erosion. Caries Res 44(3):309–316. https://doi.org/10.1159/000315932

Khan MSM et al (2013) Biodegradable waste to biogas: renewable energy option for the Kingdom of Saudi Arabia. Int J Innov Appl Stud 4(1):101–113

Konstantinou IK et al (2004) TiO_2-assisted photocatalytic degradation of azo dyes in aqueous solution: kinetic and mechanistic investigations: a review. Appl Catal B 49(1):1–14. https://doi.org/10.1016/j.apcatb.2003.11.010

Kumar SD et al (2014) Preliminary study on the dye removal efficacy of immobilized marine and freshwater microalgal beads from textile wastewater. Afr J Biotechnol. https://doi.org/10.5897/ajb2013.13242

Lade H et al (2015) Mineralization and detoxification of the carcinogenic azo dye congo red and real textile effluent by a polyurethane foam immobilized microbial consortium in an upflow column bioreactor. Int J Environ Res Public Health 12(6):6894–6918. https://doi.org/10.3390/ijerph120606894

Lin J et al (2009) Comparison between linear and non-linear forms of pseudo-first-order and pseudo-second-order adsorption kinetic models for the removal of methylene blue by activated carbon. Front Environ Sci Eng China 3(3):320–324. https://doi.org/10.1007/s11783-009-0030-7

Megha V et al (2015) Optimization of different parameters on synthetic dye decolorization by free and immobilized mucor hiemalis Mv04 (Kr078215). Res J Chem Sci 5(6):20–27

Moghaddam HM et al (2015) Fabrication of novel TiO_2 nanoparticles/Mn (Iii) salen doped carbon paste electrode: application as electrochemical sensor for the determination of hydrazine in the presence of phenol. Environ Monit Assess 187(7):407. https://doi.org/10.1007/s10661-015-4629-9

Muhammad I et al (2014) Microbial biotechnology for decolorization of textile wastewaters. Environ Sci Biotechnol 14(1):73–92. https://doi.org/10.1007/s11157-014-9344-4

Niemczynowicz J (1999) Urban hydrology and water management-present and future challenges. Urban water 1(1):1–14. https://doi.org/10.1016/s1462-0758(99)00009-6

Popli S et al (2015) Destruction of azo dyes by anaerobic-aerobic sequential biological treatment: a review. Int J Environ Sci Technol 12(1):405–420. https://doi.org/10.1007/s13762-014-0499-x

Rahimi R et al (2012) Degradation of rhodamine B using Cr-doped TiO_2 under visible light irradiation. ECSOC-16 11:1–9. https://doi.org/10.3390/ecsoc-16-01138.

Ramya M et al (2007) Biodecolorization and biodegradation of reactive blue by *Aspergillus* Sp. Afr J Biotechnol. https://doi.org/10.5897/AJB2007.000-2203

Rice EW, Baird RB, Eaton AD, Clesceri LS (2012) American public health association (APHA), standard methods for the examination of water and wastewater, American water works association (AWWA) and Water environment federation (WEF)

Roy A et al (2018) Antimicrobial and toxicological behavior of montmorillonite immobilized metal nanoparticles. Mater Sci Eng C 93:704–715

Senan RC et al (2004) Bioremediation of textile azo dyes by aerobic bacterial consortium aerobic degradation of selected azo dyes by bacterial consortium. Biodegradation 15(4):275–280. https://doi.org/10.1023/B:BIOD.0000043000.18427.0a

Shanmugam V et al (2015) Green grasses as light harvesters in dye sensitized solar cells. Spectrochim Acta Part A Mol Biomol Spectrosc 135:947–952. https://doi.org/10.1016/j.saa.2014.07.096

Shaw TE et al (2011) Eczema prevalence in the United States: data from the 2003 National Survey of Children's Health. J Investig Dermatol 131(1):67–73. https://doi.org/10.1038/jid.2010.251

Siegel FR (2002) Environmental geochemistry of potentially toxic metals. Springer, Berlin

Skouteris G et al (2015) The effect of activated carbon addition on membrane bioreactor processes for wastewater treatment and reclamation—a critical review. Bioresour Technol 185:399–410

Tapabashi NO et al (2019) Study of thermodynamic and kinetic adsorption of azo dyes on different adsorbent surfaces. Kirkuk Univ J Sci Stud 14(2):273–296

Utilization of adsorption and/or liquid membranes techniques in treatment of some hazardous substances. Ph. D., Fac. of Science, Ain Shams Univ

Wesenberg D et al (2003) White-rot fungi and their enzymes for the treatment of industrial dye Effluents. Biotechnol Adv 22(1–2):161–187. https://doi.org/10.1016/j.biotechadv.2003.08.011

Whitehead PG et al (2009) A review of the potential impacts of climate change on surface water quality. Hydrol Sci J 54(1):101–123. https://doi.org/10.1623/hysj.54.1.101

Wu Z et al (2017) Asvspoof: the automatic speaker verification spoofing and countermeasures challenge. IEEE J Sel Top Signal Process 11(4):588–604. https://doi.org/10.1109/JSTSP.2017.2671435

Yang XQ et al (2009) Decolorization of azo, triphenylmethane and anthraquinone dyes by a newly isolated *Trametes* Sp. Sq01 and its laccase. Process Biochem 44(10):1185–1189. https://doi.org/10.1016/j.procbio.2009.06.015